DOI: 10.1002/stco.70024

José Osvaldo Ferreira Filho, Luís Simões da Silva, Trayana Tankova, Hermes Carvalho

ARTICLE

General formulation for uniform and non-uniform high-strength steel slender I-section beams

The Ayrton–Perry approach is the basis of Eurocode 3 rules for buckling resistance, with distinct curves and imperfection factors depending on section type, steel grade, and other parameters. For generic members – built-up or not, uniform or not, with complex supports or not – the code allows either the general method (clause 8.3.4 of Eurocode 3) or advanced numerical simulations. Yet, the general method shows wide scatter and often underestimates resistance, while numerical analyses are time-consuming and strongly user-dependent. To overcome these limitations, the general formulation was introduced by Tankova et al. (2018) for members with variable geometry, loads, and supports and recently extended to mono-symmetric I-beams. However, it has only been validated for Class 1 and 2 sections, not for Class 4. This paper extends the general formulation to uniform and non-uniform slender I-section beams subjected to arbitrary loads, boundary conditions, and partial lateral restraints. An advanced numerical model, calibrated against experimental data, was employed to conduct a comprehensive parametric study considering different cross-sections, a range of normalized slenderness values, S460 and S690 steel grades, and different load applications. The proposal was compared with the numerical results, demonstrating a safe-sided and well-calibrated solution for the buckling resistance of high-strength steel slender I-section beams.

Keywords lateral-torsional buckling; high-strength steel; slender sections; Eurocode 3

1 Introduction

The second generation of Eurocode 3 (EC3) [1] introduces the lateral-torsional buckling (LTB) method developed by Taras and Greiner [2], as an alternative to the general case for doubly symmetric I-section beams with fork supports. The method provides accurate predictions and has been extended to monosymmetric I-sections [3], but it is not applicable to members with arbitrary boundary conditions or variable cross-sections along the length. For these cases, EC3 recommends the general method, which has been reported in the literature [4, 5] as inconsistent and computationally demanding due to its reliance on nonlinear analyses.

In response, Tankova et al. [6] introduced a general formulation (GF) for the assessment of generic members, including non-uniform cases. The approach is design-oriented, relies solely on linear buckling analysis (LBA), and has been extended to mono-symmetric I-sections [7]. However, its validation is restricted to compact and semicompact sections, with slender sections yet to be investigated.

Slender steel I-section beams fabricated from welded steel plates are commonly employed in bridge and industrial applications. The progressive availability of high-strength steel (HSS), with yield strengths two to three times higher than conventional steels while maintaining adequate ductility, weldability, and quality control, further enhances the efficiency and competitive-ness of such solutions.

The present study extends the general formulation to uniform and non-uniform slender I-section beams under uniform bending. The buckling resistance of S460 and S690 HSS members with varying cross-sections and slenderness submitted to different load distributions is assessed through a calibrated numerical model. The resulting predictions are compared with analytical solutions from the general case (GC) and general method (GM) in EC3 [1], as well as from the extended general formulation, to evaluate the accuracy and applicability of each approach.

2 Extension of the general formulation for slender sections

The general formulation (GF) implements the Ayrton–Perry design philosophy through a linear interaction equation incorporating first- and second-order normal stresses, without applying the global reduction factor, χ. No additional calibration of parameters, such as critical location or load factors, is required. The critical buckling mode from a prior linear buckling analysis (LBA) defines the initial imperfection shape, and the corresponding eigenvalues – critical load multiplier, α_{cr}, transverse displacements along the z-axis, w_{cr}, and y-axis, v_{cr}, and twist

Tab. 1 Cross-sectional properties specified by the class of the section

Class	Area A_i	Moment of inertia $I_{y,i}$	Moment of inertia $I_{z,i}$	Section modulus $W_{y,i}$	Section modulus $W_{z,i}$
1	A	I_y	I_z	$W_{\mathrm{pl},y}$	$W_{\mathrm{pl},z}$
2	A	I_y	I_z	$W_{\mathrm{pl},y}$	$W_{\mathrm{pl},z}$
3	A	I_y	I_z	$W_{\mathrm{el},y}$	$W_{\mathrm{el},z}$
4	A_{eff}	$I_{y,\mathrm{eff}}$	$I_{z,\mathrm{eff}}$	$W_{\mathrm{eff},y}$	$W_{\mathrm{eff},z}$

rotation, θ_{cr} – are used to compute second-order effects. The resulting interaction equation should be applied to all potential failure modes, and verification must be performed at a sufficient number of cross-sections along the member, including the ends.

The utilization ratio of a generic member is computed by dividing the total longitudinal stress, σ – resulting from first- and second-order effects, including axial force, $N(x)$; out-of-plane bending moments, $M_z(x)$ and $M_z^{\mathrm{II}}(x)$; in-plane bending moments, $M_y(x)$ and $M_y^{\mathrm{II}}(x)$; and bi-moment, $M_{\mathrm{w}}^{\mathrm{II}}(x)$ – by the yield stress, f_{y}. Verification of a member with arbitrary geometry, boundary conditions, and loading is performed by ensuring that Eq. (1) is satisfied.

$$\frac{N(x)}{A_i(x)\,f_{\mathrm{y}}} + \frac{M_y(x)}{W_{y,i}(x)\,f_{\mathrm{y}}} + \frac{M_z(x)}{W_{z,i}(x)\,f_{\mathrm{y}}} + \frac{M_y^{\mathrm{II}}(x)}{W_{y,i}(x)\,f_{\mathrm{y}}} + \frac{M_z^{\mathrm{II}}(x)}{W_{z,i}(x)\,f_{\mathrm{y}}} + \frac{M_{\mathrm{w}}^{\mathrm{II}}(x)}{W_{\mathrm{w}}(x)\,f_{\mathrm{y}}} \leq 1.0 \tag{1}$$

where $A_i(x)$ is the relevant cross-section area, $W_{y,i}(x)$ and $W_{z,i}(x)$ are the relevant section moduli relative to the y- and z-axes, respectively, which are defined according to Tab. 1 extracted from clause 8.2.2.6 of EC3 [1], and $W_{\mathrm{w}}(x)$ is the warping modulus at location x along the member obtained according Eq. (2).

$$W_{\mathrm{w}}(x) = \frac{I_{\mathrm{w}}(x)}{w_{\max}(x)} \tag{2}$$

where $I_{\mathrm{w}}(x)$ is the warping constant and $w_{\max}(x)$ is the maximum sectorial area.

Unlike Tankova et al. [6] and Gomes Jr. et al. [7], which considered only compact and semi-compact sections, this study includes Class 4 cross-sections. Therefore, the effective section properties (Fig. 1) are computed to account for local buckling effects.

Differently from Eurocode 3, where the designers are obligated to pre-select the relevant buckling mode a priori to the verification, the general formulation dismisses the need of identifying the buckling mode beforehand, since the all three potential critical displacements – $w_{\mathrm{cr}}(x)$, $v_{\mathrm{cr}}(x)$, and $\theta_{\mathrm{cr}}(x)$ – cannot simultaneously occur. Consequently, the resistance verification aligns with a specific buckling case.

Regarding the lateral-torsional buckling, the components of the critical buckling mode shape are $v_{\mathrm{cr}}(x)$ and $\theta_{\mathrm{cr}}(x)$, and the general interaction shown in Eq. (1) is simplified by (3):

$$\frac{M_y(x)}{W_{y,i}(x)\,f_y} + \frac{M_z^{\mathrm{II}}(x)}{W_{z,i}(x)\,f_y} + \frac{M_{\mathrm{w}}^{\mathrm{II}}(x)}{W_{\mathrm{w}}(x)\,f_y} \leq 1.0 \tag{3}$$

where the second-order contributions from $M_z^{\mathrm{II}}(x)$, which depends on the lateral displacement, $v(x)$ and the bi-moment, $M_{\mathrm{w}}^{\mathrm{II}}(x)$, which depends on the twist rotation, $\theta(x)$, are calculated using Eqs. (4) and (5).

$$M_z^{\mathrm{II}}(x) = -EI_{z,i}(x)\,v''(x) \tag{4}$$

$$M_w^{\mathrm{II}}(x) = -EI_{\mathrm{w}}(x)\,\theta''(x) \tag{5}$$

For tapered beams, an additional warping component from the inclination of the flanges appears leading the Eq. (5) to:

$$M_w^{\mathrm{II}}(x) = -EI_{\mathrm{w}}(x)\left[\theta''(x) + \frac{2}{h}\theta'(x)\,h'\right] \tag{6}$$

For simply supported beams, the amplitude can be determined through the coupling of lateral displacement and twist rotation [2, 8]. However, in a more complex configuration involving variations in geometry along the member, diverse boundary and loading conditions, etc., this relationship may not remain valid. Consequently,

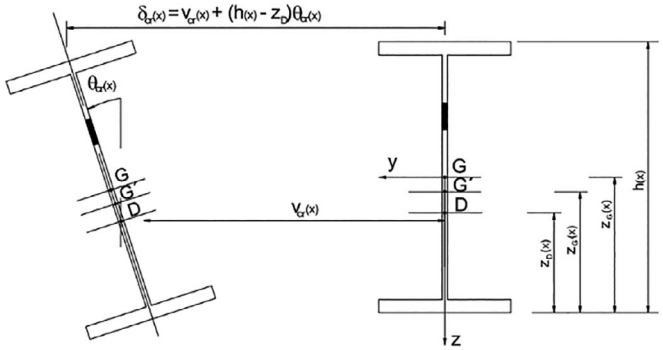

Fig. 1 Typical slender I-section and general displacement of the critical mode

it was decided to adopt both components of the mode shape as initial imperfections, assuming that they are scaled by the same amplitude. Then, the initial transverse displacement along y-axis, $v_0(x)$, and the initial twist rotation, $\theta_0(x)$, are calculated using Eqs. (7) and (8), respectively:

$$v_0(x) = v_{cr}(x)\,\bar{\delta}_{0,\mathrm{LTB}} \tag{7}$$

$$\theta_0(x) = \theta_{cr}(x)\,\bar{\delta}_{0,\mathrm{LTB}} \tag{8}$$

The resulting amplification relationship for the displacement along y-axis, $v(x)$, and twist rotation, $\theta(x)$, is:

$$v(x) = \frac{1}{\alpha_{cr}-1}\,v_0(x) \tag{9}$$

$$\theta(x) = \frac{1}{\alpha_{cr}-1}\,\theta_0(x) \tag{10}$$

Assuming that the real beam has the same buckling resistance as an equivalent simply supported beam, with the same geometry at the critical cross-section, x_m, and the same elastic critical bending moment, equalling the second-order utilization factors for both, it is possible to obtain the required generalized imperfection. It is further assumed that the location x_m is the location where $|v''_{cr}|$ is maximum along the beam.

The second-order utilization factor for the equivalent beam at the critical cross-section, x_m, is given by:

$$\begin{aligned}\varepsilon_M^{II}(x_m) &= \frac{M_z^{II}(x_m)}{W_{z,i}(x_m)\,f_y} + \frac{M_w^{II}(x_m)}{W_w(x_m)\,f_y}\\ &= \frac{\alpha_{cr} M_{y,Ed}(x_m)\,\bar{e}_0\theta_{cr}(x_m)}{W_{z,i}(x_m)\,f_y(\alpha_{cr}-1)}\\ &\left(1+\frac{v_{cr}(x_m)}{\theta_{cr}(x_m)}\frac{W_{z,i}(x_m)}{W_w(x_m)}+\frac{GJ(x_m)}{M_{cr}}\frac{W_{z,i}(x_m)}{W_w(x_m)}\right)\\ &= \frac{N_{cr,z,eq}\bar{e}_0}{W_{z,i}(x_m)\,f_y(\alpha_{cr}-1)}\end{aligned} \tag{11}$$

From Eqs. (4), (5), and (6), the second-order utilization factor for the real beam at the same location is expressed by:

$$\begin{aligned}\varepsilon_M^{II}(x_m) &= \frac{M_z^{II}(x_m)}{W_{z,i}(x_m)\,f_y} + \frac{M_w^{II}(x_m)}{W_w(x_m)\,f_y} =\\ &\frac{EI_{z,i}(x_m)\,\bar{\delta}_0}{W_{z,i}(x_m)\,f_y(\alpha_{cr}-1)}\left[v''_{cr}(x_m)+\frac{W_{z,i}(x_m)}{W_w(x_m)}\frac{I_w(x_m)}{I_{z,i}(x_m)}\right.\\ &\left.\left(\theta''_{cr}(x_m)+\frac{2}{h}\theta'_{cr}(x_m)\,h'\right)\right]\bar{\delta}_0\end{aligned} \tag{12}$$

For slender sections with Class 3 and 4 webs and compact flanges, Eq. (12) becomes:

$$\begin{aligned}\varepsilon_M^{II}(x_m) &= \frac{M_z^{II}(x_m)}{W_{z,i}(x_m)\,f_y} + \frac{M_w^{II}(x_m)}{W_w(x_m)\,f_y}\\ &= \frac{EI_z(x_m)\left(v''_{cr}(x_m)+\frac{h}{2}\theta''_{cr}(x_m)+\theta'_{cr}(x_m)\,h'\right)\bar{\delta}_0}{W_z(x_m)\,f_y(\alpha_{cr}-1)}\end{aligned} \tag{13}$$

As:

$$\frac{W_{z,i}(x_m)}{W_w(x_m)}\,\frac{I_w(x_m)}{I_{z,i}(x_m)} = \frac{\frac{I_{z,i}(x_m)}{\frac{b}{2}}I_w(x_m)}{\frac{I_w(x_m)}{w_{max}(x)}I_{z,i}(x_m)} = \frac{\frac{2}{b}}{\frac{4}{hb}} = \frac{h}{2} \tag{14}$$

Equaling Eqs. (11) and (13) yields the amplitude of the imperfection related to lateral-torsional buckling, $\bar{\delta}_{0,\,\mathrm{LTB}}$ (Eq. (15)), that contains the equivalent geometrical imperfection, $\bar{e}_0$, and additional terms establishing the consistency with Eurocode 3 [1] stability design rules.

$$\begin{aligned}\bar{\delta}_{0,\mathrm{LTB}} &= \frac{N_{cr,z}\bar{e}_0}{EI_{z,i}(x_m)\left[v''_{cr}(x_m)+\frac{h}{2}\theta''_{cr}(x_m)+\theta'_{cr}(x_m)\,h'\right]}\\ &= f_\eta\,\bar{e}_0\end{aligned} \tag{15}$$

Following [6], $\bar{e}_0$ is given by Eq. (16):

$$\bar{e}_0 = \alpha_{LT}(x_m)\left(\bar{\lambda}(x_m)-0.2\right)f_\eta\left|\delta_{cr}(x_m)\right|\frac{W_{z,i}(x_m)}{A_i(x_m)} \tag{16}$$

where $\alpha_{LT}(x_m)$ is the imperfection factor related to the lateral-torsional buckling from EN 1993-1-1 [4], $\bar{\lambda}(x_m)$ is the nondimensional slenderness at a given position, the factor f_η is given by Eq. (17), and $\delta_{cr}(x_m)$ is the general displacement of the critical mode found by a geometric relationship between the lateral displacement and the rotation of the section (Fig. 1), which is expressed by Eq. (18).

$$f_\eta = \frac{N_{cr,z,eq}}{EI_{z,i}(x_m)\left[v''_{cr}(x_m)+\frac{h}{2}\theta''_{cr}(x_m)+\theta'_{cr}(x_m)\,h'\right]} \tag{17}$$

$$\delta_{cr}(x_m) = v_{cr}(x_m) + (h(x_m) - z_D)\,\theta_{cr}(x_m) \tag{18}$$

Finally, the utilization ratio $\varepsilon_M(x)$ can be expressed by:

$$\begin{aligned}\varepsilon_M(x) &= \frac{M_{y,Ed}(x)}{W_{y,i}(x)\,f_y}\\ &+\frac{EI_{z,i}(x)\left[v''_{cr}(x)+\frac{h}{2}\theta''_{cr}(x_m)+\theta'_{cr}(x_m)\,h'\right]}{A_i(x)\,f_y(\alpha_{cr}-1)}\,\eta(x)\le 1.0\end{aligned} \tag{19}$$

With:

$$\eta(x) = \alpha_{LT}(x)\left(\bar{\lambda}(x)-0.2\right)f_\eta\left|\delta_{cr}(x)\right| \tag{20}$$

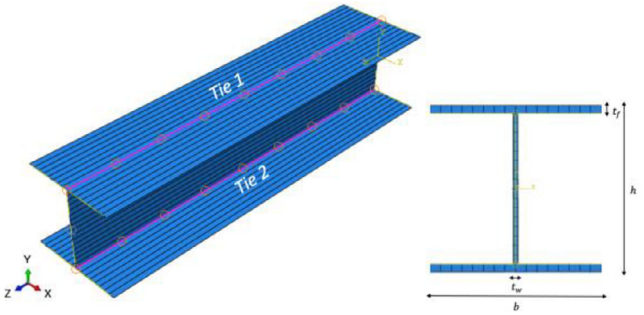

Fig. 2 Cross-section, assembly of the model and application of tie constraints

Using the differential equation for flexural buckling in Eq. (21), the equivalent elastic critical force for out-of-plane buckling, $N_{cr,z,eq}$, is "retrieved" in Eq. (22):

$$\mathrm{EI}_{z,i}(x)\, v''_{cr}(x) + N_{cr,z,eq} v_{cr}(x) = 0 \tag{21}$$

$$N_{cr,z,eq} = \frac{\mathrm{EI}_{z,i}(x_m)\left|v''_{cr}(x_m)\right|}{\left|v_{cr}(x_m)\right|} \tag{22}$$

This force is the one used herein for the calculation of the normalized slenderness in Eq. (23):

$$\bar{\lambda}(x) = \sqrt{\frac{A_i(x)\, f_y}{N_{cr,z,eq}}} \tag{23}$$

3 Numerical model

3.1 Description

The numerical model was developed in ABAQUS [9] as an extension for beams from the mod-el proposed by Ferreira Filho et al. [10]. The geometry was defined using nominal dimensions, and overlaps at the web-flange junctions were eliminated through tie constraints, ensuring proper connectivity. Fig. 2 presents the reference geometry and key parameters. Longitudinal welds between the web and flanges were omitted without compromising accuracy, consistent with previous findings [11].

Tab. 2 Experimental versus numerical results of resistance

Prototype	Ult. resistance (kN)		*FEM*
	EXP	**FEM**	***EXP***
B5	1024.5	1018.3	0.99
B7	1384.6	1395.2	1.01
B8	1327.9	1329.2	1.00
B11	1731.8	1822.7	1.05
B12	1601.0	1620.1	1.01
B13	1307.2	1331.4	1.02
B14	1133.3	1142.8	1.01

The material's true stress-strain response was defined following the non-linear hardening model from EC3-1-14 [12]. The four-node fully integrated shell element S4 was employed, with a mesh consisting of 16 elements across the flange width and 16 across the web depth, consistent with prior studies [11].

The fork boundary conditions were modelled following the recommendations of Snijder et al. [13]. Lateral and vertical displacements, as well as torsional rotations, were constrained at the centroid nodes of the end sections. At one end, longitudinal displacements were additionally restrained at the centroid node (Fig. 3a). At both ends, all flange nodes were coupled to their mid-node for displacements and rotations, while web nodes were similarly coupled except for rotations about the vertical axis, enabling infinitely rigid but warpable end sections (Fig. 3b). End bending moments were applied at the centroid nodes.

Initial geometric imperfections were introduced using the LTB eigenmode obtained from lin-ear buckling analyses (LBA), with an amplitude of $L/1000$ in accordance with ECCS recom-mendations [14]. The distribution and magnitude of membrane residual stresses followed the

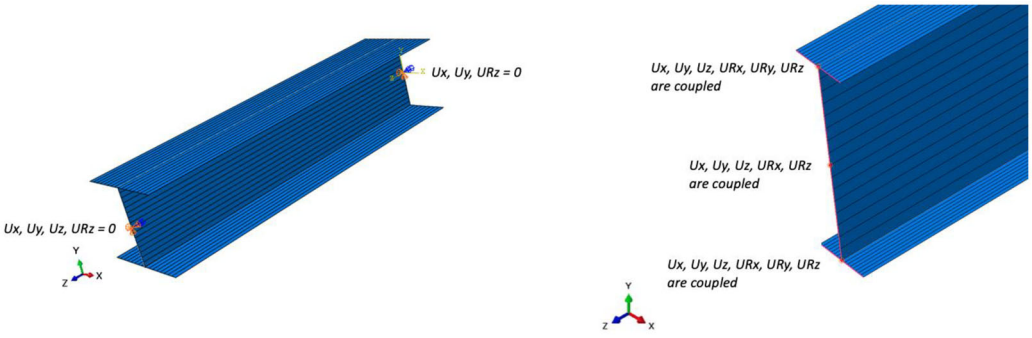

(a) Boundary conditions (b) Constraints

Fig. 3 Simulation of fork supports

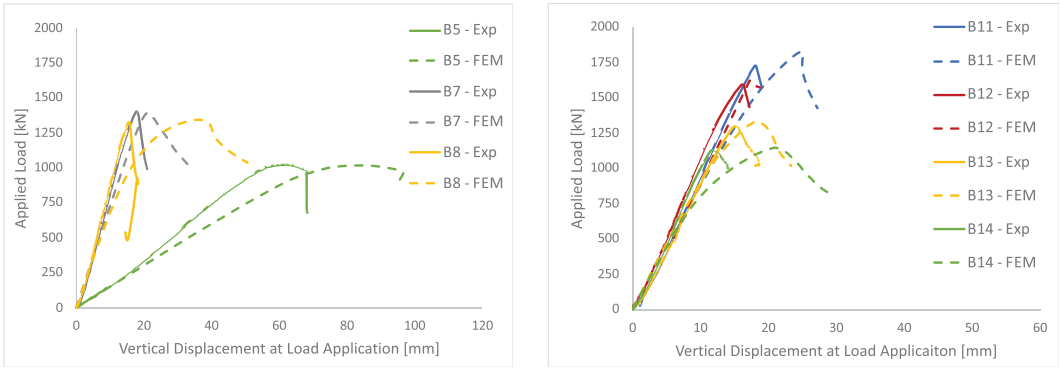

(a) Doubly-symmetric (b) Mono-symmetric

Fig. 4 Comparison between load versus displacement curves of the beams

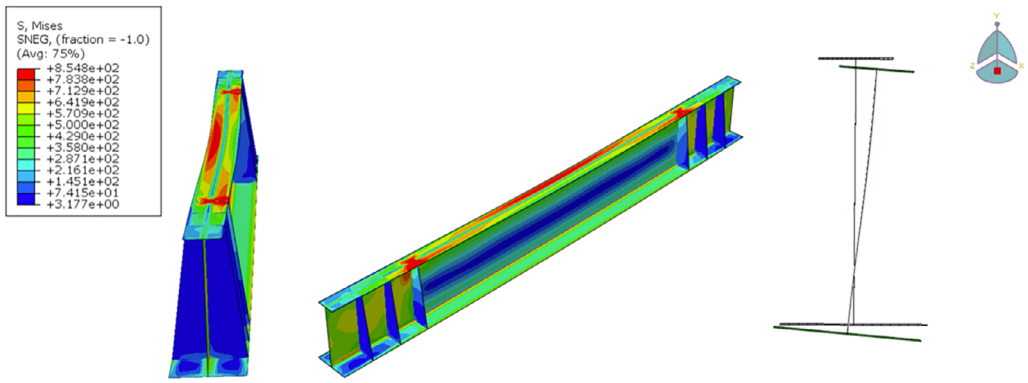

Fig. 5 Reproduced lateral-torsional buckling failure mode (example of the prototype B11)

model proposed by Schaper et al. [15] for welded I-section members with thermally cut flanges.

3.2 Validation

The numerical model was validated against experimental results from class 4 welded I-section beams tested in the STROBE project [16], where details about the member properties are reported. Deviations are presented in Tab. 2, showing good agreement between numerical and experimental results. A consistent correlation was also observed between vertical load-displacement curves (Fig. 4). Moreover, the numerical model reproduced the expected experimental failure modes (Fig. 5).

3.3 Parametric study

A parametric study was conducted on uniform and non-uniform Class 4 I-section beams of HSS grade S460 and S690 (Tab. 3) subjected to different load distribution

Tab. 3 S460 and S690 HSS beams covered in the parametric study

Type	Steel grade	Section 1 $h \times b \times t_w \times t_f$ [mm]	Section 2 $h \times b \times t_w \times t_f$ (mm)	h_1/h_2
Uniform	S460 and S690	700 × 200 × 8 × 16	700 × 200 × 8 × 16	1.00
Uniform	S460 and S690	850 × 200 × 8 × 16	850 × 200 × 8 × 16	1.00
Uniform	S460 and S690	925 × 200 × 8 × 16	925 × 200 × 8 × 16	1.00
Uniform	S460 and S690	1000 × 200 × 8 × 16	1000 × 200 × 8 × 16	1.00
Non-uniform	S690	850 × 200 × 8 × 16	700 × 200 × 8 × 16	1.21
Non-uniform	S690	925 × 200 × 8 × 16	700 × 200 × 8 × 16	1.32
Non-uniform	S690	1000 × 200 × 8 × 16	700 × 200 × 8 × 16	1.43
Non-uniform	S690	925 × 200 × 8 × 16	850 × 200 × 8 × 16	1.16
Non-uniform	S690	1000 × 200 × 8 × 16	850 × 200 × 8 × 16	1.25
Non-uniform	S690	1000 × 200 × 8 × 16	925 × 200 × 8 × 16	1.08

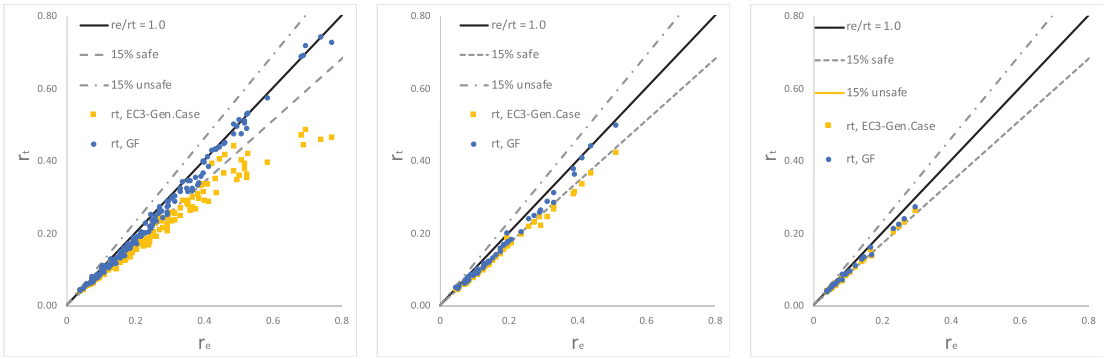

(a) End moment distribution (b) Distributed load (c) Point load

Fig. 6 Comparison between numerical results and analytical results from GF and EC3 for uniform beams

(bending moment distribution with the ratio between the maximum and minimum, ψ, equal to −1, 0, or 1; distributed load and point load). The S460 and S690 HSS grades were covered and members ranging from stocky to slender were analyzed, with nondimensional slenderness, $\bar{\lambda}_z$, varying between 1.0 and 7.0.

4 Validation of the general formulation for slender I-section beams

The results from the numerical model were compared against the analytical results from the general formulation (GF) and EC3 [1]. Scatter plots of r_t versus r_e are presented for all sections, where r_e denotes the ratio of numerical to plastic resistance and r_t the ratio of analytical to plastic resistance. In Fig. 6, the plots for the uniform beams are sectored by each type of load. The results were statistically evaluated in terms of ratios r_N between the numerical and analytical buckling resistances: an average r_N equal to 1.26 with c.o.v. of 8.7% is found for EC3 while an average r_N equal to 1.12 with c.o.v. of 6.5% for GF. When comparing GC from EC3 and GF, the poor performance of GC stems directly from the lack of mechanical consistency in the derivation of this method.

The scatter plots for the non-uniform S690 slender I-section beams submitted to end bending moment distribution are shown in Fig. 7. The results were also statistically assessed in terms of ratios r_N: an average r_N equal to 1.44 with c.o.v. of 7.6% is found for GM from EC3 while an average r_N equal to 1.18 with c.o.v. of 6.3% for GF.

5 Conclusion

This study confirmed the potential of the general formulation (GF) to provide consistent and safe-sided predictions for the stability design of uniform and non-uniform HSS slender I-section beams. Comparisons against numerical results highlighted the superior accuracy of GF over the EC3 approaches, particularly in capturing the mechanical

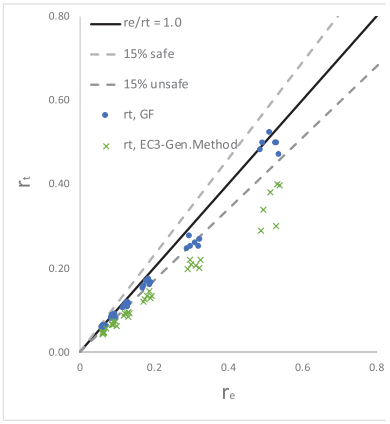

Fig. 7 Comparison between numerical results and analytical results from GF and EC3 for non-uniform beams

behavior under different loading and boundary conditions. While the present investigation demonstrated the robustness of GF for the cases covered herein, further studies are recommended to extend its field of application to a wider range of cross-sections, additional steel grades, stockier members, and broader boundary conditions. Moreover, a calibration of the method is necessary to ensure that the safety margins are consistent with the fundamental requirements of EN 1990. Finally, it should be noted that distortional buckling is not covered in the present study; therefore, future research should address members susceptible to this mode of failure.

6 Annex - Flowchart for the application of the general formulation

The procedure for applying the general formulation to the design of beams potentially susceptible to lateral-torsional buckling is outlined in the flowchart presented in Fig. A1.

As a first step, the user should identify the critical buckling mode and its associated load factor, α_{cr}, and critical displacements, v_{cr} and θ_{cr}, through a linear buckling analysis.

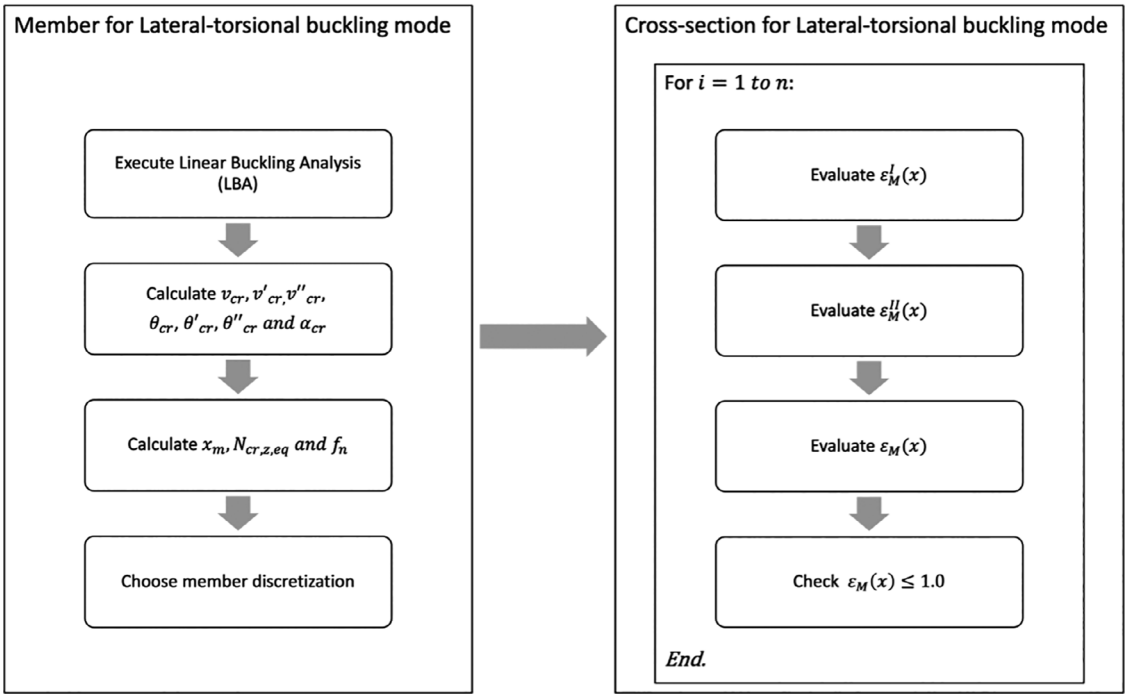

Fig. A1 Application of the general formulation for the lateral-torsional buckling of uniform and non-uniform beams

Secondly, the critical location, x_m, is defined as the location where $|v''_{cr}|$ is maximum and the equivalent elastic critical force, $N_{cr,z,eq}$, is calculated by Eq. (22).

The member is then discretized in "n" elements along its length. The utilization ratio, $\varepsilon_M(x)$, is verified at these specified locations according to the first order forces from the bending moment diagram along the member. Finally, the global utilization ratio, $\varepsilon_M(x)$, for the lateral-torsional buckling mode is determined using Eq. (19), and the member is verified.

Acknowledgements

– FCT/MCTES through national funds (PIDDAC) under the R&D Unit Institute for Sustainability and Innovation in Structural Engineering (ISISE), under reference UIDB/04029/2020 https://doi.org/10.54499/UIDB/04029/2020), and under the Associate Laboratory Advanced Production and Intelligent Systems (ARISE) under reference LA/P/0112/2020.

– The doctoral grant 2021.06106.BD by the Portuguese Foundation for Science and Technology (FCT) attributed to the first author.

– The Brazilian National Council for Scientific and Technological Development (CNPq) under the project n° 446626/2024-4 and the grant n° 314913/2025-4 attributed to the first author.

Open access publication funding provided by FCT (b-on).

References

[1] EN 1993-1-1 (2022) *Eurocode 3 - Design of Steel Structures – Part 1-1: General Rules and Rules for Buildings*. Brussels: Comité Européen de Normalisation (CEN).

[2] Taras, A.; Greiner, R. (2010) *New design curves for lateral-torsional buckling – proposal based on a consistent derivation*. Journal of Constructional Steel Research 66, No. 5, pp. 648–663.

[3] Simões da Silva, L.; Gomes Junyor, J. O.; Ferreira Filho, J. O.; Carvalho, H. (2025) *Ayrton-Perry approach for the lateral-torsional buckling resistance of mono-symmetric I-section beams*. Thin-Walled Structures 211, p. 113125. https://doi.org/10.1016/j.tws.2025.113125

[4] Marques, L. et al. (2013) *Development of a consistent design procedure for lateral-torsional buckling of tapered beams*. Journal of Constructional Steel Research 89, pp. 213–235.

[5] Simões da Silva, L.; Marques, L.; Rebelo, C. (2010) *Numerical validation of the general method in EC3-1-1: lateral, lateral-torsional and bending and axial force interaction of uniform members*. Journal of Constructional Steel Research 66, pp. 575–590. https://doi.org/10.1016/j.jcsr.2009.11.003

[6] Tankova, T.; Simões da Silva, L.; Marques, L. (2018) *Buckling resistance of non-uniform steel members based on stress utilization: general formulation*. Journal of Constructional Steel Research 149, pp. 239–256.

[7] Gomes Jr. J. O. et al. (2023) *Lateral-torsional buckling resistance of non-prismatic and prismatic monosymmetric I-section steel beams based on stress utilization*. Engineering

Structures 305, p. 117758. https://doi.org/10.1016/j.engstruct.2024.117758
[8] Chen, F.; Astuta, T. (1977) *Theory of beam-columns Vol. 2: Space behaviour and design*. McGraw-Hill, New York.
[9] Abaqus v. 6.21. (2021) Providence, RI, USA: Dassault Systems/Simulia.
[10] Ferreira Filho, J. O. et al. (2022) *Experimental and numerical flexural buckling resistance of high strength steel columns and beam-columns*. Engineering Structures 265, p. 114414. https://doi.org/10.1016/j.engstruct.2022.114414
[11] Ferreira Filho, J. O.; Simões da Silva, L.; Tankova, T.; Carvalho, H. (2023) *Influence of geometrical imperfections and residual stresses on the reliability of high strength steel welded I-section columns using Monte Carlo simulation*. Journal of Constructional Steel Research 215, p. 108548. https://doi.org/10.1016/j.jcsr.2024.108548
[12] prEN 1993-1-14. (2022) *Eurocode 3: Design of steel structures – Part 1-14: Design assisted by finite element analysis*. Brussels: Comité Européen de Normalisation (CEN).
[13] Snijder, H. H.; van der A. R. P.; Hofmeyer, H.; van Hove, B. W. E. M. (2018) *Lateral torsional buckling design imperfections for use in non-linear FEA*. Steel Construction 11, pp. 49–56. https://doi.org/10.1002/stco.201810015
[14] ECCS (1984) *Ultimate Limit State Calculation of Sway Frames with Rigid Joints*. Brussels: Publication No.33.
[15] Schaper, L.; Tankova, T.; Simões da Silva, L.; Knobloch, M. (2022) *A novel residual stress model for Welded I-sections*. Journal of Constructional Steel Research 188, p. 107017.
[16] Tankova, T. et al. (2021) *Lateral-torsional buckling of high strength steel beams: Experimental resistance*. Thin-Walled Structures 164, p. 107913.

Authors

Professor Dr. José Osvaldo Ferreira Filho (corresponding author)
joffilho.ct@uem.br
State University of Maringá (UEM)
Department of Civil Engineering
Colombo Av., 5790, Bloco C67 – Zona 7
87020-900 Maringá - Paraná
Brazil

Prof. Dr. Luís Simões da Silva
luisss@dec.uc.pt
University of Coimbra (UC)
ISISE, ARISE, Department of Civil Engineering
Luis Reis dos Santos St., 290
3030, 790 Coimbra
Portugal

Prof. Dr. Trayana Tankova
t.tankova@tudelft.nl
Delft University of Technology (TUDelft)
Department of Engineering Structures
Mekelweg 5
2628 CD Delft
Netherlands

Prof. Dr. Hermes Carvalho
hermes@dees.ufmg.br
Federal University of Minas Gerais (UFMG)
Department of Structural Engineering
Presidente Antônio Carlos Av., 6627, Escola de Engenharia - Pampulha
31270 – 901 Belo Horizonte – Minas Gerais
Brazil

How to Cite this Paper
Ferreira Filho, J. O.; Simões da Silva, L.; Tankova, T.; Carvalho, H. (2026) *General formulation for uniform and non-uniform high-strength steel slender I-section beams*. Steel Construction 19, No. 2, pp. 171–178.
https://doi.org/10.1002/stco.70024

This paper has been peer reviewed. Submitted: 25 September 2025; accepted: 31 January 2026.